

# Molecular Mass Transportation Via Carbon Nanoscrolls

Yinjun Huang

Teng Li<sup>1</sup>

e-mail: LiT@umd.edu

Department of Mechanical Engineering,  
University of Maryland,  
College Park, MD 20742

The open topology of a carbon nanoscroll (CNS) inspires potential applications such as high capacity hydrogen storage. Enthusiasm for this promising application aside, one crucial problem that remains largely unexplored is how to shuttle the hydrogen molecules adsorbed inside CNSs. Using molecular dynamics simulations, we demonstrate two effective transportation mechanisms of hydrogen molecules enabled by the torsional buckling instability of a CNS and the surface energy induced radial shrinkage of a CNS. As these two mechanisms essentially rely on the nonbonded interactions between the hydrogen molecules and the CNS, it is expected that similar mechanisms could be applicable to the transportation of molecular mass of other types, such as water molecules, deoxyribonucleic acids (DNAs), fullerenes, and nanoparticles. [DOI: 10.1115/1.4024167]

Keywords: carbon nanoscrolls, molecular mass transportation, buckling, hydrogen storage

## 1 Introduction

A carbon nanoscroll is formed by rolling up a graphene sheet into a spiral nanostructure. A CNS is topologically open, thus its core size can be tuned by relative sliding between adjacent layers. By contrast, a carbon nanotube (CNT) is topologically closed; therefore, the radius of a CNT can only be modestly increased by stretching and deflecting the carbon-carbon (C-C) covalent bonds. The highly tunable structure of CNSs has inspired research efforts to explore their potential applications [1–11]. Previous studies have found that CNSs have great potential for hydrogen storage [2–4]. Particularly, the spiral structure of a CNS can be further opened by alkali doping, thus allowing the CNS to accommodate more hydrogen than a CNT [4]. Enthusiasm for this promising application aside, one crucial problem that remains largely unexplored is how to make effective molecular mass transportation through CNSs. For example, it remains elusive how to shuttle the hydrogen molecules adsorbed inside CNSs. It is desirable to explore an effective molecular mass transportation mechanism to enable the future application of CNS-based hydrogen storage.

Mass transportation through CNTs has been studied in recent years [12–16]. A few approaches have been demonstrated experimentally or theoretically. For example, various species of molecules (e.g., hydrogen and DNA) can be transported using a CNT in torsion and compression [12,15]; transportation of water molecules can be realized by a CNT pump with a small portion of initially twisted wall [14]; gas flow can be conducted inside CNT by Rayleigh traveling waves on the tube surface [16].

Inspired by these research progresses and taking into account the open and highly tunable structure of CNSs, in this paper we use molecular dynamics (MD) simulations to investigate two effective mechanisms of molecular hydrogen transportation enabled by (a) the torsional buckling instability of CNSs and (b) surface energy induced radial shrinking of CNSs.

## 2 Adsorption of Hydrogen Into a CNS

We first use MD simulation to demonstrate the physisorption of hydrogen molecules into a CNS. The CNS in the MD simulation has a length of 8 nm and inner core diameter of 2 nm (perspective view shown in Fig. 1(a)). The second-generation reactive empiri-

cal bond order potential [17] and 12-6 Lennard-Jones potential [18] are adopted to describe the C-C covalent interaction and van der Waals (vdW) force, respectively. The CNS is initially immersed in a hydrogen reservoir to achieve hydrogen adsorption (Fig. 1(a)). To simulate the hydrogen physisorption on the CNS, the hydrogen-carbon vdW interaction is also described by 12-6 Lennard-Jones potential  $V_{CH}(r) = 4\epsilon_{CH}((\sigma_{CH}^{12}/r^{12}) - (\sigma_{CH}^6/r^6))$ , where  $r$  is the hydrogen-carbon atomic pair distance,  $\epsilon_{CH} = 2.998 \times 10^{-3}$  eV, and  $\sigma_{CH} = 3.18$  nm [19]. Note that chemisorption of hydrogen molecules on the CNS could also occur [20], which can potentially lead to a higher hydrogen storage capacity, while only physisorption is considered in this study. The simulation is carried out using large-scale atomic/molecular massively parallel simulator (LAMMPS) [21] with canonical ensemble at a temperature of 70 K and a time step of 0.001 picosecond (ps). Driven by the concentration gradient, hydrogen molecules are shown to enter the CNS structure and then be physically adsorbed inside the CNS due to the vdW adhesion. Figures 1(b)–1(d) shows sequential snapshots of the end view of the CNS with hydrogen physisorption at 50 ps, 150 ps, and 250 ps, respectively. After about 300 ps, the hydrogen physisorption into the CNS reaches equilibrium, with 572 hydrogen molecules adsorbed and adhered to the inner walls of CNS, corresponding to a gravimetric hydrogen uptake of 1.56 wt. %. It is also interesting that hydrogen molecules adsorbed inside the CNS core form a spiral structure in extension of the CNS structure, similar to the previous findings of water molecules confined inside a CNS core [7].

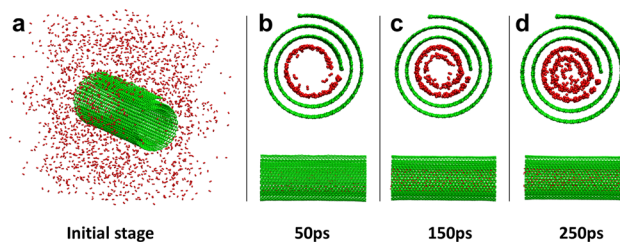
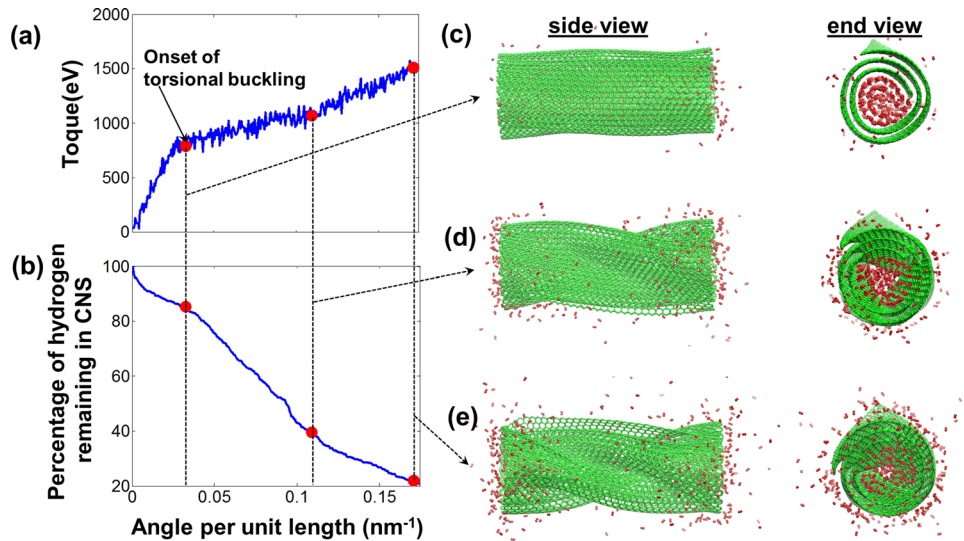


Fig. 1 (a) Perspective view of a CNS immersed in a hydrogen reservoir. (b)–(d) Sequential snapshots of the end view (top) and side view (bottom) of the CNS with hydrogen physisorption at 50 ps, 150 ps, and 250 ps, respectively. For visual clarity, hydrogen molecules outside of the CNS are not shown. A simulation video showing the hydrogen molecule physisorption into a CNS is available at <http://ter.ps/h2adsp>.

<sup>1</sup>Corresponding author.

Manuscript received January 7, 2013; final manuscript received February 5, 2013; accepted manuscript posted April 8, 2013; published online May 31, 2013. Editor: Yonggang Huang.



**Fig. 2** (a) Resultant torque as a function of twisting angle per unit length for the CNS immersed in a hydrogen reservoir. The change of slope indicates the onset of torsional buckling. (b) Percentage of hydrogen molecules remaining inside the CNS as a function of twisting angle per unit length. After the occurrence of torsional buckling, the collapse of the CNS squeezes more adsorbed hydrogen molecules out of the CNS, as indicated by the change of slope of the curve. (c)–(e) The side and end views of the CNS and the hydrogen molecules initially adsorbed inside the CNS inner core at the onset of torsional buckling (0.03 rad/nm) and at a twisting angle of 0.105 rad/nm and 0.17 rad/nm, respectively. For visual clarity, the hydrogen molecules initially outside of the CNS are not shown. A simulation video showing the hydrogen molecule transportation enabled by torsional buckling of the CNS is available at <http://ter.ps/h2bkl>.

### 3 Molecular Hydrogen Transportation Enabled by Torsional Buckling of the CNS

Recent studies of the buckling instability of CNSs [22] reveal that the torsional buckling of a CNS is distinct from that of a CNT of similar size. Dictated by the open topology of the CNS, the critical buckling loading of a CNS is much lower than that of a CNT of similar size. Furthermore, the torsional buckling of a CNS occurs in a much more gradual manner compared to the abrupt buckling process of a CNT under torsion. Such a feature is desirable to achieve a smooth molecular mass transportation. In this section, we demonstrate molecular hydrogen transportation enabled by torsional buckling of a CNS.

To achieve the transportation of the adsorbed hydrogen molecules through the CNS, a torsional deformation along the length direction up to 0.17 rad/nm is gradually applied to the CNS by fixing the left end of and twisting its right end with a loading rate of  $5.45 \times 10^{-4}$  rad/nm/ps. The torsional buckling of the CNS and the associated transportation process of hydrogen adsorbed in the CNS are illustrated in Fig. 2.

The evolution of the amount of the adsorbed hydrogen molecules remaining inside the CNS is presented as a function of the applied torsional deformation (Fig. 2(b)). Initial deformation causes the tightening of the CNS, reducing the cross section area, which in turn imposes a stronger repulsive vdW force on the hydrogen molecules. As a result, some hydrogen molecules are pushed out of the CNS. Upon further application of the torsional loading, the CNS buckles when the deformation reaches 0.031 rad/nm. At this stage, 14.5% of the adsorbed hydrogen molecules are squeezed out of the CNS. Note that the onset of torsional buckling of the CNS (Fig. 2(a)) is much more gradual than that of a CNT of similar size, which is often indicated by a sharp drop of the resultant torque at the onset of buckling [22]. As torsional buckling develops, much more adsorbed hydrogen molecules are transported through the CNS as indicated by a steeper slope of the curve in Fig. 2 beyond the onset of buckling. At the end of the loading, 79.4% of the hydrogen molecules initially

adsorbed inside the CNS are squeezed out of the CNS, suggesting the high efficacy of the molecular transport by torsional buckling instability of the CNS. In this simulation, a relatively short CNS is used, to which torsion may be challenging to apply in a real situation. A long CNS, however, buckles more easily under torsion, and the hydrogen inside can eventually be pushed out as the deformation of the CNS wall continues to develop. Therefore, the hydrogen transport mechanism demonstrated here still holds. A bundle of CNSs subject to torsion can also lead to the molecular mass transport in a similar fashion but could be more realistic to achieve in experiment.

To investigate the effect of loading rate on the efficacy of torsional buckling enabled molecular mass transportation, we performed MD simulations at four different loading rates of  $2.725 \times 10^{-4}$  rad/nm/ps,  $5.45 \times 10^{-4}$  rad/nm/ps,  $1.09 \times 10^{-3}$  rad/nm/ps, and  $2.18 \times 10^{-3}$  rad/nm/ps, respectively. Figure 3 plots the percentage of hydrogen molecules remaining inside the CNS as a function of twisting angle per unit length for these four cases. It is shown that the total amount of hydrogen molecules squeezed out of the CNS increases modestly as the loading rate gets lower.

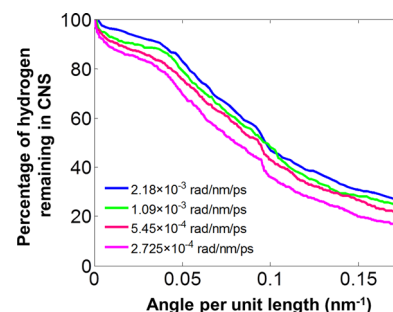


**Fig. 3** Percentage of hydrogen molecules remaining inside the CNS as a function of twisting angle per unit length for four different loading rates

This can be understood as follows. At a low loading rate, the development of the buckling deformation of the CNS becomes more gradual, which in turn allows the transportation of the hydrogen molecules to be smoother, and thereby the vdW interactions between carbon and hydrogen can play a more effective role in facilitating the mass transportation. Nonetheless, the molecular mass transportation mechanism enabled by torsional buckling instability is shown to be robust over a range of loading rates.

#### 4 Molecular Hydrogen Transportation Enabled by Surface Energy Induced Radial Shrinking of a CNS

Next we demonstrate another mechanism to achieve molecular mass transportation via CNSs. Unlike the closed tubular structure of a CNT, the open spiral structure of a CNS indicates that the CNS core size may be tuned by external stimuli [7,20]. Energetically, the equilibrium shape of a CNS (and thus its core size) is governed by the competition between the surface energy and scrolling-associated strain energy of the basal graphene. It has been shown that the core radius of a CNS is dependent on the surface energy, the C–C interlayer spacing, the bending stiffness, and the length of its basal graphene [9]. Particularly, an increased surface energy of the basal graphene can balance more scrolling-associated strain energy of the basal graphene and, therefore, result in a tighter CNS with a smaller core radius at equilibrium. In other words, the inner core size of a CNS can be varied if the surface energy of its basal graphene can be tunable. For example, it has been shown that an applied electric field can lead to the polarization of the carbon atoms in a CNS, which in turn results in dipole–dipole interaction energy [7]. Therefore, the effective surface energy of the CNS consists of the contribution of both the C–C vdW interaction energy and the dipole–dipole interaction energy. As a result, the effective surface energy of the CNS can be varied by changing the applied electric field, and consequently, the core size of the CNS can be tuned over a broad range. Such a tunable core size of the CNS has been shown to facilitate tunable water transport [7]. In this section, we use MD simulations to demonstrate molecular hydrogen transportation enabled by radial shrinking of a CNS due to the change of surface energy of the basal graphene.

To simulate the collective effect of surface energy on the CNS morphology, a tuning factor  $\lambda$  is introduced in the nonbonded Lennard–Jones potential to represent the change in effective surface energy. The carbon–carbon interaction is thereby described by a Lennard–Jones pair potential  $V_{CC}(r) = 4\lambda\epsilon_{CC}((\sigma_{CC}^{12}/r^{12}) - (\sigma_{CC}^6/r^6))$ , where  $r$  is the C–C atomic pair distance,  $\epsilon_{CC} = 2.844 \times 10^{-3}$  eV, and  $\sigma_{CC} = 3.4$  nm. To capture the associated change in the hydrogen–carbon nonbonded interaction, the Lorentz–Berthelot mixing rules [23] are applied so that the hydrogen–carbon interaction is given by a Lennard–Jones pair potential  $V_{CH}(r) = 4\sqrt{\lambda}\epsilon_{CH}((\sigma_{CH}^{12}/r^{12}) - (\sigma_{CH}^6/r^6))$ , where  $r$  is the hydrogen–carbon atomic pair distance,  $\epsilon_{CH} = 2.998 \times 10^{-3}$  eV, and  $\sigma_{CH} = 3.18$  nm.

A CNS with hydrogen molecules adsorbed inside its core as described in Sec. 2 is used as the starting configuration in the simulation. The simulation is carried out with canonical ensemble at a temperature of 70 K and a time step of 0.001 ps. We first set  $\lambda$  to be 7. The increased surface energy of the basal graphene leads to a tighter CNS structure; therefore, the core shrinking of the CNS drives the transportation process of hydrogen adsorbed inside the CNS. Such a process is illustrated in Fig. 4.

When an increase surface energy of the basal graphene is exposed at the beginning of the simulation, the CNS shrinks as the original equilibrium interlayer spacing no longer corresponds to the minimum energy state. As shown in Fig. 4, at  $t=5$  ps, the CNS has already tightened a little bit with a few hydrogen molecules squeezed out from the ends of the CNS. The CNS continues tightening with its core size shrinking until  $t=20$  ps, at which time about 65% of the adsorbed hydrogen molecules are pushed out of the CNS. The hydrogen transportation process here is

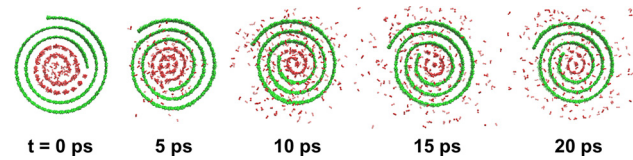


Fig. 4 Sequential snapshots of the hydrogen molecules initially adsorbed inside a CNS being squeezed out of the CNS due to the radial shrinkage of the CNS driven by a sudden increase of the surface energy of the basal graphene. For visual clarity, the hydrogen molecules initially outside of the CNS are not shown. A simulation video showing the hydrogen molecule transportation enabled by radial shrinkage of the CNS is available at <http://ter.ps/h2shrkr>.

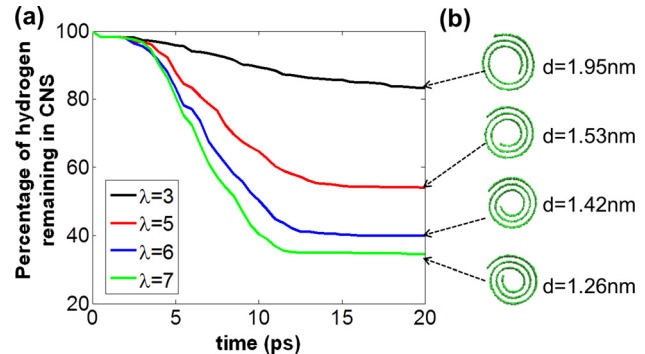


Fig. 5 (a) Percentage of hydrogen molecules remaining inside the CNS as a function of simulation time for four different tuning factors of surface energy of the basal graphene. (b) End view and resultant inner core diameter of the CNS at the end of the simulation for each case. For visual clarity, hydrogen molecules are not shown.

essentially driven by the shrinking core size of the CNS, which is in turn governed by the surface energy of the basal graphene. To reveal the quantitative dependence of the efficiency of molecular mass transportation on the change of surface energy, we conduct further simulations with a set of tuning factors of surface energy ( $\lambda = 3, 5, 6,$  and  $7$ ) and compare the results in Fig. 5.

It shows that the larger the change in the surface energy of the basal graphene, the faster the CNS core shrinking process attains its equilibrium as indicated by the relatively earlier transition to the plateau regime of the curves in Fig. 5. Also emerging from Fig. 5 is that as the change in the effective surface energy increases, the efficiency of the hydrogen molecule transportation improves, which can be understood by the smaller resultant core size of the CNS for a higher surface energy of the basal graphene. For example, as shown in the simulation results, the resultant core diameters of the CNS for  $\lambda = 3, 5, 6, 7$  are 1.95 nm, 1.53 nm, 1.42 nm, and 1.26 nm, respectively (Fig. 5(b)). The simulation results in this section show that radial shrinkage of a CNS by tuning the surface energy of its basal graphene could be another potential effective mechanism of molecular mass transportation via CNSs.

#### 5 Concluding Remarks

In summary, using MD simulations, we demonstrate two effective hydrogen molecule transportation mechanisms via CNSs enabled by the torsional buckling instability of the CNS and surface energy induced radial shrinkage of the CNS. It is shown that a high efficacy of hydrogen molecule transportation up to about 80% can be achieved by leveraging the torsional buckling instability of the CNS and such a transportation mechanism is robust

over a range of torsional loading rates. If a sufficiently large change in the surface energy of the basal graphene can be achieved, the resulting radial shrinkage can also lead to hydrogen molecule transportation with a reasonable efficacy. As the two transportation mechanisms demonstrated in this paper are essentially driven by the nonbonded interaction of the hydrogen molecules and the basal graphene of the CNS, it is expected that the similar mechanisms are applicable for the transportation of molecular mass of other types, such as water molecules, DNAs, fullerenes, and nanoparticles. While the simulation results presented here are promising, there are challenges that are crucial for the experimental realization of the demonstrated molecular mass transportation mechanisms. For example, it remains largely unexplored how to manipulate a CNS with sufficient precision to apply mechanical loads and how to significantly tailor the surface energy of a CNS without severely compromising the structural integrity of the basal graphene. We therefore call for further experimental explorations of the molecular mass transportation mechanisms envisioned by the present study.

### Acknowledgment

This research is supported by the U.S. National Science Foundation (Grant Nos. 1069076 and 1129826).

### References

- [1] Braga, S. F., Coluci, V. R., Legoas, S. B., Giro, R., Galvão, D. S., and Baughman, R. H., 2004, "Structure and Dynamics of Carbon Nanoscrolls," *Nano Lett.*, **4**(5), pp. 881–884.
- [2] Coluci, V. R., Braga, S. F., Baughman, R. H., and Galvão, D. S., 2007, "Prediction of the Hydrogen Storage Capacity of Carbon Nanoscrolls," *Phys. Rev. B*, **75**(12), p. 125404.
- [3] Braga, S. F., Coluci, V. R., Baughman, R. H., and Galvão, D. S., 2007, "Hydrogen Storage in Carbon Nanoscrolls: An Atomistic Molecular Dynamics Study," *Chem. Phys. Lett.*, **441**(1–3), pp. 78–82.
- [4] Mpourmpakis, G., Tyliaakis, E., and Froudakis, G. E., 2007, "Carbon Nanoscrolls: A Promising Material for Hydrogen Storage," *Nano Lett.*, **7**(7), pp. 1893–1897.
- [5] Shi, X., Pugno, N. M., Cheng, Y., and Gao, H., 2009, "Gigahertz Breathing Oscillators Based on Carbon Nanoscrolls," *Appl. Phys. Lett.*, **95**(16), p. 163113.
- [6] Xie, X., Ju, L., Feng, X., Sun, Y., Zhou, R., Liu, K., Fan, S., Li, Q., and Jiang, K., 2009, "Controlled Fabrication of High-Quality Carbon Nanoscrolls From Monolayer Graphene," *Nano Lett.*, **9**(7), pp. 2565–2570.
- [7] Shi, X., Cheng, Y., Pugno, N. M., and Gao, H., 2010, "Tunable Water Channels With Carbon Nanoscrolls," *Small*, **6**(6), pp. 739–744.
- [8] Zhang, Z., and Li, T., 2010, "Carbon Nanotube Initiated Formation of Carbon Nanoscrolls," *Appl. Phys. Lett.*, **97**(8), p. 081909.
- [9] Shi, X. H., Pugno, N. M., and Gao, H. J., 2010, "Mechanics of Carbon Nanoscrolls: A Review," *Acta Mech. Solida Sinica*, **23**(6), pp. 484–497.
- [10] Shi, X., Cheng, Y., Pugno, N. M., and Gao, H., 2010, "A Translational Nanoactuator Based on Carbon Nanoscrolls on Substrates," *Appl. Phys. Lett.*, **96**(5), p. 053115.
- [11] Zhang, Z., and Li, T., 2011, "Ultrafast Nano-Oscillators Based on Interlayer-Bridged Carbon Nanoscrolls," *Nanoscale Res. Lett.*, **6**, p. 470.
- [12] Wang, Q., 2009, "Transportation of Hydrogen Molecules Using Carbon Nanotubes in Torsion," *Carbon*, **47**(7), pp. 1870–1873.
- [13] Wang, Q., 2009, "Atomic Transportation Via Carbon Nanotubes," *Nano Lett.*, **9**(1), pp. 245–249.
- [14] Duan, W. H., and Wang, Q., 2010, "Water Transport With a Carbon Nanotube Pump," *ACS Nano*, **4**(4), pp. 2338–2344.
- [15] Wu, N., Wang, Q., and Arash, B., 2012, "Ejection of DNA Molecules From Carbon Nanotubes," *Carbon*, **50**(13), pp. 4945–4952.
- [16] Insepov, Z., Wolf, D., and Hassanein, A., 2006, "Nanopumping Using Carbon Nanotubes," *Nano Lett.*, **6**(9), pp. 1893–1895.
- [17] Brenner, D. W., Shenderova, O. A., Harrison, J. A., Stuart, S. J., Ni, B., and Sinnott, S. B., 2002, "A Second-Generation Reactive Empirical Bond Order (REBO) Potential Energy Expression for Hydrocarbons," *J. Phys. Condens. Matter*, **14**(4), pp. 783–802.
- [18] Stuart, S. J., Tutein, A. B., and Harrison, J. A., 2000, "A Reactive Potential for Hydrocarbons With Intermolecular Interactions," *J. Chem. Phys.*, **112**(14), pp. 6472–6486.
- [19] Gu, C., Gao, G. H., Yu, Y. X., and Mao, Z.-Q., 2001, "Simulation Study of Hydrogen Storage in Single Walled Carbon Nanotubes," *Int. J. Hydrogen Energy*, **26**(7), pp. 691–696.
- [20] Zhou, B., Guo, W. L., and Tang, C., 2008, "Chemisorption of Hydrogen Molecules on Carbon Nanotubes: Charging Effect From First-Principles Calculations," *Nanotechnology*, **19**(7), p. 075707.
- [21] Plimpton, S., 1995, "Fast Parallel Algorithms for Short-Range Molecular-Dynamics," *J. Comput. Phys.*, **117**(1), pp. 1–19.
- [22] Zhang, Z., Huang, Y., and Li, T., 2012, "Buckling Instability of Carbon Nanoscrolls," *J. Appl. Phys.*, **112**(6), p. 063515.
- [23] Allen, M. P., and Tildesley, D. J., 1987, *Computer Simulation of Liquids*, Clarendon, Oxford, UK.